The Effect of Processing Conditions on the Mechanical Properties of Polypropylene/Mesoporous Silica-Hydroxyapatite Hybrid Nanocomposites

A.R. Albooyeh [a]*, S. Tarahomi [b], A.B. Fereidoon [b], Z. Taherian [c]

[a] *School of Engineering, Damghan University, Damghan, Iran*
[b] *Department of Mechanical Engineering, Semnan University, Semnan, Iran*
[c] *Department of Materials Engineering, Semnan University, Semnan, Iran*

PAPER INFO

ABSTRACT

This work focused on the influence of processing conditions on the mechanical properties of polypropylene (PP) and PP/mesoporous silica-hydroxyapatite (PP/MCM-41-HA) hybrid nanocomposites. The mechanical properties of PP were enhanced by adding MCM-41-HA nanoparticles. Neat PP and hybrid nanocomposites based on PP, containing maleic anhydride-grafted polypropylene (PP-g-MA) and MCM-41-HA, were prepared using the melt intercalation technique in an internal mixer. To optimize the processing conditions, both mixing temperature and rotor rotational speed were varied. Tensile and flexural tests were performed to evaluate some mechanical characteristics (stress-strain curves, tensile strength, tensile modulus, strain at rupture, flexural strength. and flexural modulus) of both the neat PP and PP/ MCM-41-HA hybrid nanocomposite materials. The results showed that two of the materials' mechanical properties were most affected by two preparation parameters: shear rate and the distribution process of nanocomposites were found to be optimized using a mixing temperature of 180° C and a rotor rotational speed of 100 rpm to achieve the best mechanical properties. Under these conditions, the best mixing time was 3 min according to the torque diagram. Moreover, the PP/MCM-41-HA hybrid nanocomposite demonstrated a sensible enhancement of mechanical properties over neat PP.

1. Introduction

Mesoporous silica nanofillers have received much attention due to their ordered structure, high surface area, and ease of use of the nanopores [1]. Among them, extensive research has been performed on MCM-41 with a hexagonal array of one-dimensional channels of uniform mesoporous silica with pore diameters in the range of 2–10 nm [2, 3]. Low hydrothermal stability of MCM-41 materials undoubtedly limits their application, which is thought to improve strength by increasing the thickness of the pore walls and/or by enhancing the local ordering of the walls [4]. Combining two nanomaterials with different shapes may generate more effectively enhanced effects due to the expected synergistic effect. For example, Wang et al.

showed that nanocomposites comprised of PP/MCM-41/MMT have higher values of tensile strength, tensile modulus, and impact strength than PP/MMT or PP/MCM-41 nanocomposites [5]. Therefore, combining MCM-41 with a rigid rod shape nanoparticle, such as hydroxyapatite (HA), can enhance the pore walls and achieve greater mechanical performance.

HA is the main inorganic component of the hard tissues (bones and teeth) of vertebrate animals and humans [6]. The mechanical strength of polymers can be greatly improved by adding a small amount of these inorganic nanofillers. The mechanical properties of polymer composites reinforced with HA have been examined in several studies. Younesi and Bahrololoom investigated the effects of molecular weight and particle size on mechanical properties of

---

* Corresponding author, Tel.: +98-23-35220414; Fax: +98-23-35220414

E-mail address: a.albooyeh@du.ac.ir

PP/HA biocomposites [7]. In another study, Younesi and Bahrololoom examined the mechanical properties of PP-HA composites under applied temperature and pressure in a hot-pressing process [8]. Li and Tjong introduced nano-sized HA into PP and demonstrated that the addition of 8 wt% HA, led to an increased tensile modulus of nearly 25% [9].

Melt processing is a critical step in the manufacture of polymer articles and is even more critical when dealing with inhomogeneous polymer-mesoporous nanocomposite systems. As shown in the literature results, the changes in processing conditions greatly affected the nanocomposites' dynamic-mechanical properties [10]. Thus, the mechanical dispersing action depended on processing parameters, such as compounding equipment [11], geometry, the types of mixing elements [12], and the rheological characteristics of the polymer. Additionally, the optimal dispersion of nanocomposites can be increased by adjusting parameters, such as shear stress, mixing time, and mixing temperature [13]. Other works on the influence of processing conditions on the properties of PP nanocomposites include Furlan et al. [14], who studied the effect of processing conditions on the mechanical and thermal properties of high-impact polypropylene nanocomposites. In addition, Malaika et al. [15] studied the influence of processing and clay type on nanostructure and the stability of polypropylene-clay nanocomposites. Luijsterburg et al. [16] researched the effects of processing conditions on structural and mechanical properties of recycled polypropylene. Recently, studies concerning the effects of processing conditions on the mechanical and morphological properties of polypropylene nanocomposites have been published [17-20].

In this study, to enhance the pore walls consisting of MCM-41, HA was added to the MCM-41, and a new kind of nanocomposite MCM-41-HA was introduced and its mechanical properties were studied. Neat PP and PP/MCM-41-HA hybrid nanocomposites were prepared through melt intercalation in an internal mixer, by monitoring several processing conditions, including mixing temperatures and the rotor rotational speed, which were altered to optimize the processing conditions for combining materials. The optimum processing conditions were obtained, and they are explained in this study for the first time.

2. Materials and Methods

2.1. Materials

Polypropylene homopolymer (PP 570P), in pellet form, was obtained from the Sabic company in Saudi Arabia, consisting of the following characteristics: Melt Flow Index (MFI) = 8 g/10 min (230° C/2.16 kg), and density = 905 kg/m^3. The monodisperse nano-sized MCM-41/HA particles were synthesized in our lab. The nano-sized MCM-41 particles were prepared in an aqueous phase using the sol–gel method. The materials used in this study included $CaCl_2\_2H_2O$ (99–102%, Merck) and $K_2HPO_4\_3H_2O$ (Merck, ≥ 99%), as phosphorous and calcium sources, respectively. Cetyltrimethylammonium bromide ($C_{16}TAB$, Sigma) was used as a template, tetraethoxysilane (Merck, ≥ 99%) was used as a silicon source, and an ammonia solution (25% Merck, > 98%) as a pH controller were also used. Next, tetra-n-botylortho titanat as a titanium source, ethanol and diethanolamine were used for preparation of Titania sol-gel. Moreover, polypropylene-grafted maleic anhydride (PP-g-MA) with an MFI = 2 g/10 min from Karangin company in Iran, was employed as a compatibilizer to improve the adhesion between the PP and the nanoparticles. Surface modification and stronger chemical bonds between the nanoparticles and PP were made by coating the fillers with PP-g-MA. The PP-g-MA contained 1.7 wt% of maleic anhydride (MA).

2.2. Synthesis of HA

$K_2HPO_4\_3H_2O$ was first dissolved in 100 ml of deionized water. Then, $C_{16}TAB$ was added under magnetic stirring (500 rpm). After that, enough TMAOH was added to adjust the pH to 12. Meanwhile, in another container, $CaCl_2\_2H_2O$ was also dissolved in 100 ml deionized water, and then it was added to the prior solution under constant stirring (500 rpm). The obtained gel was aged at 30° C for 30 h under reflux and static conditions after 1 h of stirring [21].

2.3. Synthesis of the MCM-41-HA Nanocomposites

After the preparation of HA, 45 ml TEOS was added drop-wise to the solution under vigorous stirring (within about 30 min). The final solution was aged at 100° C for 36 h without stirring. The nominal composition is 60 wt% of SiO_2. The solid products were filtered, washed, and dried for 2 h at 90° C. In the next step, the solid products were calcined at 550° C for 6 h and finally were labelled as MCM-41-HA [22, 23]. The nanoparticle properties were as follows: density = 2.5 gr/cm^3; specific surface area = 280 m^2/gr; particle size = 9.71 (nm). The schematic form of mesoporous silica nanoparticles was shown in Figure 1.
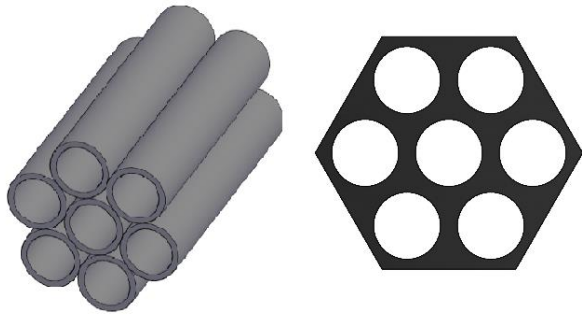
Figure 1. The schematic form of mesoporous silica nanoparticles.

2.4. Preparation of Nanocomposites

Neat PP and nanocomposites based on PP containing 3 wt% PP-g-MA and 3 wt% MCM-41-HA were prepared through melt intercalation in an internal mixer (Haake Rheomix, W50-EHT). Prior to preparation of nanocomposites, PP, MCM-41-HA, and PP-g-MA were dried in a vacuum oven at 80° C for 24 h to expel moisture. In order to optimize the mixing parameters, composites were prepared by varying the chamber temperature and rotor rotational speed. In the first step, neat PP and PP/MCM-41-HA nanocomposites were mixed with a rotor rotational speed of 50 rpm at several mixing temperatures, including 170° C, 180° C, and 200° C for a period of 5 min [13-15]. Afterwards, the mixing temperature was fixed at 180° C, and the rotor rotational speed was varied at 60 rpm, 80 rpm, and 100 rpm in the next step [13,15].

2.5. Mechanical Tests

All tensile and flexural specimens were prepared by using an injection-molding machine. Mechanical tests were performed at room temperature by means of a universal testing machine, GOTECH (Tcs-2000).

Dumbbell specimens were set up for the tensile tests, according to the ASTM: D638-10 standard using a cross-sectional area of 10 mm × 3.2 mm. A cross-head speed of 50 mm/min and a load of 100 kN were applied. Flexural tests were performed according to the ASTM: D790-10 standard, in a 3-point loading test at a speed of 10 mm/min. Cubic specimens of 100 mm × 13 mm × 5 mm were used for this test. The span length between the supports was 80 mm with a constant deflection rate at the loading point. The mechanical properties were reported as the average of at least five measurements.

2.6. Morphological Study

X-ray diffraction (XRD) and a scanning electron microscope (SEM) were used to examine the mor-phological properties and dispersion state of MCM-41-HA in nanocomposites.

The XRD patterns of samples were recorded, using both a Bruker D8 tools diffractometer with Cu Kα radiation and a small-angle X-ray diffraction with a Philips X'Pert diffractometer at λ= 0.15406 nm and a scan rate of 0.07°. The diffractometer was operated at 35 kV and 30 mA.

The samples were cut from each specimen, followed by immersion in liquid nitrogen. Prior to testing the surfaces of the specimens were coated with a thin gold layer (Emitec, 450-kx, UK) and then were detected using SEM (VEGA.TESCA, Czech Republic).

3. Results and Discussion

3.1. Mechanical Properties

As previously mentioned, in melt-mixed nanocomposites, the properties of the system are dependent on mixing conditions, such as mixing time, rotor rotational speed, and the mixing temperature. These parameters have been optimized by preparing a set of neat PP and PP/MCM-41-HA nanocomposites by changing the rotor rotational speed and mixing temperature, and choosing the best mixing time from a torque diagram. Tensile and flexural tests were performed to evaluate the effect of processing conditions on the mechanical properties of neat PP and the PP/MCM-41-HA nanocomposite.

In the first step, the rotor rotational speed was fixed at 50 rpm, and the mixing temperature was varied at 170° C, 180° C, and 200° C. Tensile and flexural properties of neat PP and PP/MCM-41-HA nanocomposites at the different temperatures are shown in Figure 2.

Figure 2 shows that the tensile and flexural properties of neat PP were not dependent on the temperature. In the PP/MCM-41-HA nanocomposite specimens, these properties increased with the increase in temperature from 170° C to 180° C but decreased with the increase to 200°. Therefore, the maximum values for the nanocomposite specimens' tensile and flexural strength occurred at 180° C.

Figure 2 illustrates that at the optimum mixing temperature (180° C), a significant improvement in tensile and flexural properties occurred. At that temperature, the enhancement of the tensile properties for PP/MCM41-HA nanocomposite was about 7% (43.37 MPa versus 40.52 MPa) for tensile strength and 13% (1515 MPa versus 1341 MPa) for tensile modulus. In addition, the improvement values for flexural strength were about 15% (44.02 MPa versus 38.48 MPa) and for flexural modulus were 17% (1468 MPa versus 1261 MPa).

At low temperatures, the viscosity, related to the shear stress generated in the mixture, is very high, and this causes the break down of MCM-41-HA nanoparticles during mixing. Thus, at the temperature of 170° C, tensile and flexural properties were reduced when compared with the properties at a mixing temperature of 180° C. The decrease of mechan-

ical properties at a mixing temperature of 200° C could be due to the thermal degradation of MCM-41-HA nanoparticles, or the dispersion of MCM-41-HA nanoparticles in the PP matrix being poor due to the decreased viscosity at a higher temperature. These results are consistent with other studies [13, 15].
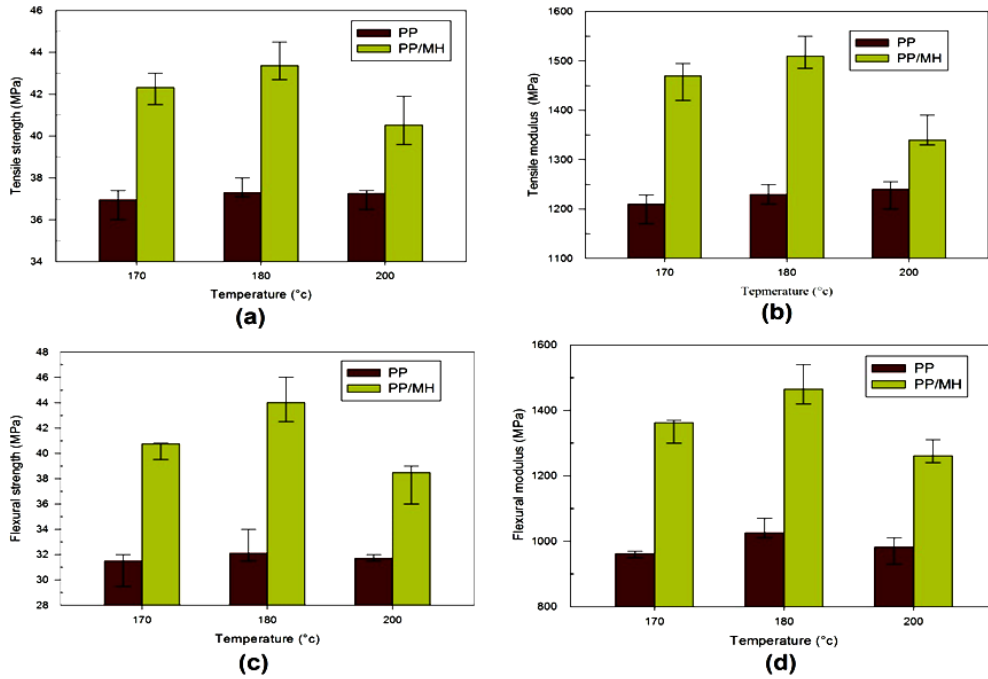

Figure 2. The effect of mixing temperature on the mechanical properties of neat PP and a PP/MCM-41-HA nanocomposite: (a) tensile strength, (b) tensile modulus, (c) flexural strength, (d) flexural modulus.

Figure 3. The effect of rotor rotational speed on the mechanical properties of neat PP and a PP/MCM-41-HA nanocomposite: (a) tensile strength, (b) tensile modulus, (c) flexural strength, (d) flexural modulus.
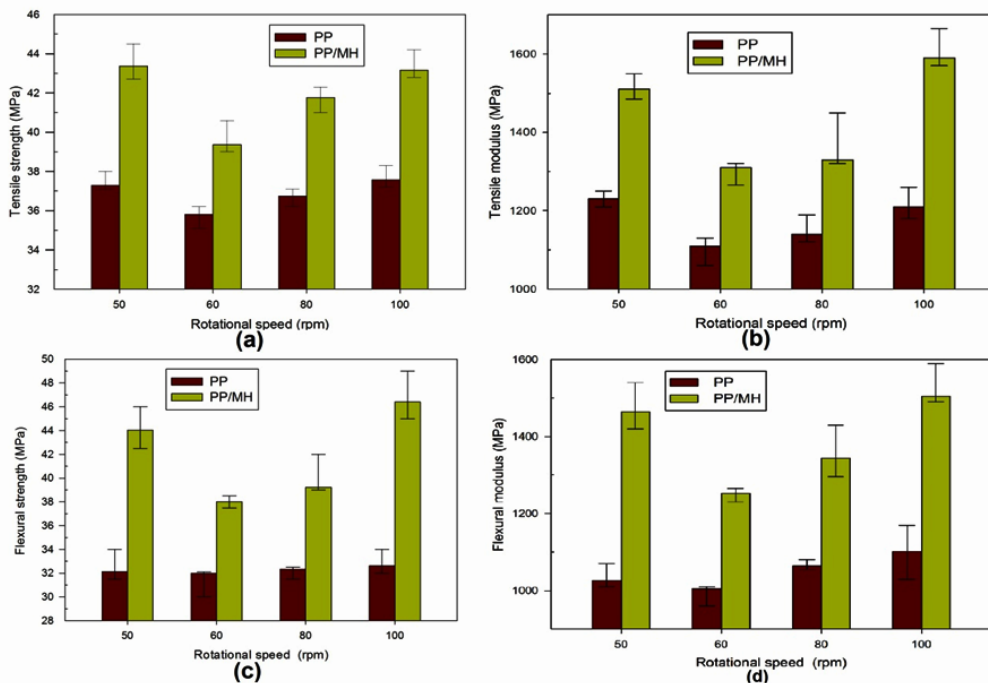
In the second step, the mixing temperature was fixed at 180° C (the optimal temperature from the previous step), and the rotor rotational speed was changed to 60 rpm, 80 rpm, and 100 rpm. The tensile and flexural properties of neat PP and PP/MCM-41-HA nanocomposites in the different rotor rotational speed (50 rpm, 60 rpm, 80 rpm, and 100 rpm) are shown in Figure 3.

Results revealed that the tensile and flexural properties of specimens decreased with the increased rotor rotational speed from 50 rpm up to 80 rpm and then the tensile and flexural properties increased at a rotor rotational speed of 100 rpm. It is obvious that the tensile and flexural properties at the rotor rotational speed of 100 rpm were higher than at the other rotor rotational speeds. At the optimal rotational speed, the enhancement of the tensile and flexural properties for PP/MCM41-HA nanocomposite was about 10% (43.16 MPa versus 39.36 MPa) for tensile strength, 22% (1597 MPa versus 1311 MPa) for tensile modulus, 23% (46.4 MPa versus 38 MPa) for flexural strength, and 21% (1505 MPa versus 1252 MPa) for flexural modulus.

Figure 2 and Figure 3 show that the sensitivity of tensile and flexural properties of neat PP with changing the mixing temperature and rotor rotational speed was trivial, because changing in the processing conditions of melt-mixing has influence on the diffusion of nanoparticles in a polymer matrix (whereas nanoparticles do not exist in neat PP). It is found that the best result in mechanical properties for neat PP and PP/MCM-41-HA nanocomposite specimens were obtained at the optimum temperature of 180° C using a rotor rotational speed of 100 rpm.

Figure 4 shows that elongation at break of neat PP and PP/MCM-41-HA nanocomposites was improved by increasing the rotational speed of the rotor. The maximum value of elongation at break happened at a rotor rotational speed of 100 rpm. Incorporation of the MCM-41-HA results in an abrupt drop in elongation at break compared with the elongation at break of neat PP, because the filler causes a reduction in matrix deformation due to an introduction of mechanical restraints [24]. On the other hand, reduction of elongation at break may be due to greater interaction between the filler and the polymer matrix, which probably led to a lower polymeric chain mobility, making the material more rigid.
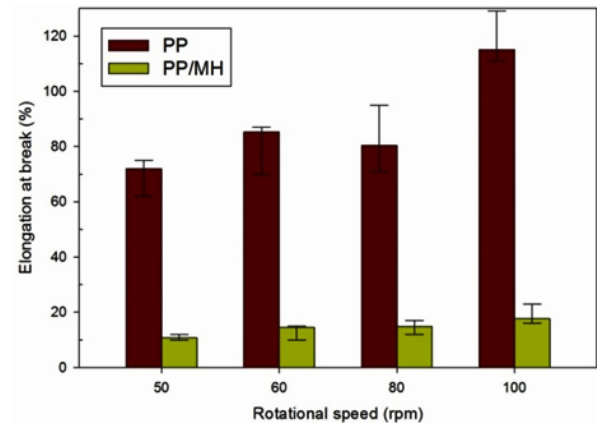

Figure 4. The effect of rotor rotational speed on the elongation at break of neat PP and a PP/MCM-41-HA nanocomposite.

The comparison of mechanical properties of neat PP with PP/MCM-41-HA nanocomposites shows that tensile strength, tensile modulus, flexural strength, and flexural modulus of PP/MCM-41-HA nanocomposites were increased, and the elongation at the break decreased in proportion to neat PP. By adding nanoparticles to the PP matrix, greater interaction occurred, and it caused a lower elongation at break and increased mechanical characteristics.

Table 1 shows the percentage increase for mechanical properties of PP/MCM-41-HA nanocomposites in proportion to neat PP. Approximately 17%, 32%, 42%, and 43% increases in tensile strength, tensile modulus, flexural strength, and flexural modulus were observed for the samples, respectively.

Adding MCM-41 to the blend allows the mixture to adsorb polymer matrix on its surface because of its high surface area. As the surface area increases, filler-matrix adhesion improved and caused an increase of mechanical performances compared to neat PP [25]. In addition, the three-dimensional MCM-41 networks provided a rigid inorganic framework that improved mechanical strength and modulus [26].

Because of the porosity of MCM-41-HA, the chains of PP form in the mesopore channels, which restrain the agglomeration of MCM-41-HA particles [5]. The PP phase in the nano-sized pores extended along the channels to the openings, which can enhance the interaction through the entanglement and inter-diffusion between the matrix and the particulate, improving the tensile and flexural properties. Moreover, the hydrophobicity properties of the nano-sized MCM-41-HA, due to the polymer on the outer surface of the MCM-41-HA particles, would improve filler/matrix miscibility [27].

High rigidity, large aspect ratio, and the mechanical interlocking effect of HA nanoparticles led to better reinforcement of PP/MCM-41-HA nanocomposites. Other researchers have reported similar results [6, 9, 28]. Adding the HA nanoparticles enhanced the pore walls of MCM-41 [4]. These features, in turn, caused the good mechanical properties seen in the PP/MCM-41-HA nanocomposite.

3.2. Torque Plot

Mixing torque is an important indicator for evaluating the processing characteristics of polymer nanocomposites, particularly when internal mixing is employed. The mixing characteristics of neat PP and PP/MCM-41-HA nanocomposites were studied by using the Haake Rheographs. These plots were carried out for the temperatures and the rotor rotational speed conditions presented in Table 1.

Considering the results for the same polymeric matrix processed using different conditions, two parameters should be analysed: the shear rate and the diffusive processes. Figure 5 shows the torque diagram versus the mixing time for the PP/MCM-41-HA nanocomposite. Since the torque diagram of neat PP is similar to that of the PP/MCM-41-HA nanocomposite, the torque diagram for neat PP was not included.

From Figure 5, it is clear that the mixing torque initially increases rapidly when PP granules and MCM-41-HA nanoparticles are charged into the mixer chamber because of the increased viscosity of the system. As the mixing time increases, PP/MCM-41-HA granules underwent melting, which resulted in the decrease of torque, and then the torque stabilized.

Table 1. Comparison of the mechanical properties of neat PP and a PP/MCM-41-HA nanocomposite.

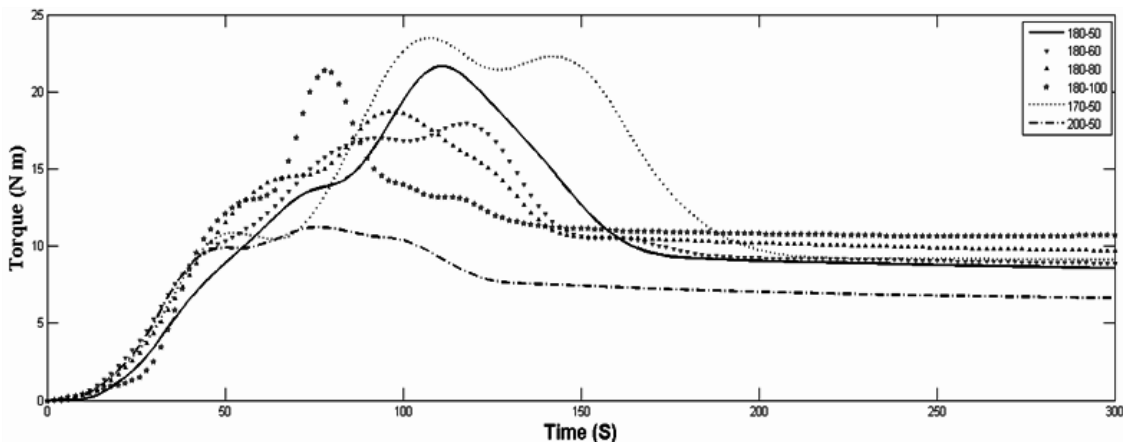| Temperature (°C)	Rotor rotational speed (rpm)	Tensile strength increase (%)	Tensile modulus increase (%)	Flexural strength increase (%)	Flexural modulus increase (%)
170	50	14.53	21.48	29.30	41.50
180	50	16.30	22.77	37.04	42.78
200	50	8.70	12.40	21.38	28.41
180	60	9.90	18.10	18.82	24.50
180	80	13.66	16.66	21.30	26.34
180	100	14.90	31.40	42.24	36.69

Figure 5. Mixing torque against the time diagram for a PP/MCM-41-HA nanocomposite.

The instant increase in torque can be attributed to the high shear forces generated by the rotor in the presence of granules just before their melting point. As the granules melt, the viscosity of the granules decreased under high temperature; consequently, the mixing torque decreased. Once the dispersion was completed, the mixture homogenized, and the torque began to stabilize.

Better results were obtained using processing conditions that maximized the shear stresses (maximized torque) and minimized the stabilization time exerted on the polymer, which occurred at higher rotational speed (100 rpm) and at a barrel profile temperature of 180° C.

Considering the results for the same chamber temperature, the increased rotor rotational speed led to increased shear stress exerted on the polymer and simultaneously decreased the required mixing time. The results revealed that the first parameter—shear stress—has much more influence on the extent of intercalation and delimitation than the second one—mixing time). Therefore, at higher rota-

tional speeds (100 rpm), the increased shear stress caused the diffusion of nanoparticles in the matrix better than a lower rotational speed (50 rpm).

3.3. Morphological Characterization

The effect of processing conditions on the dispersion of nanoparticles in a PP/MCM-41-HA nanocomposite was studied by using SEM. Figures 6(a)–(d) show the fractured surface micrographs of neat PP and 3 wt%-filled nanocomposites for three different processing conditions. These micrographs show that dispersion of MCM-41-HA was uniform and agglomeration did not happen.

Comparison between the size of nanoparticles shows that the smallest size of measured nanoparticles is about 50 nm for nanocomposites, which were produced at a chamber temperature of 180° C and a rotor rotational speed of 100 rpm, as shown in Figure 6(d). Under these conditions, due to the lower viscosity, better diffusion was obtained because the nanoparticles had enough time to diffuse within the PP matrix.
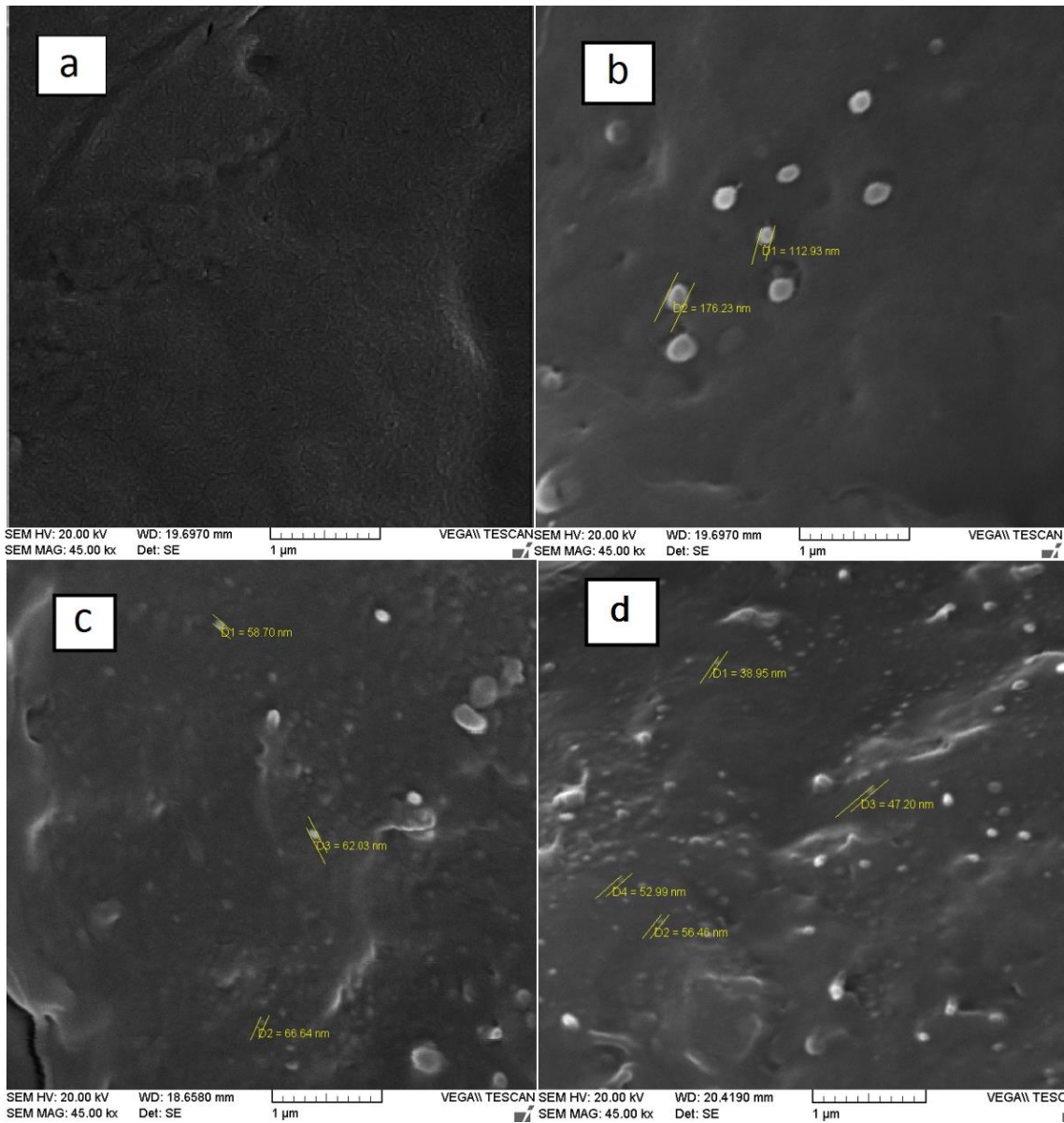

Figure 6. SEM micrographs of (a) neat PP, (b) PP/MCM-41-HA nanocomposite (temperature 170° C and rotational speed of 50 rpm), (c) PP/MCM-41-HA nanocomposite (temperature 180° C and rotational speed of 50 rpm), (d) PP/MCM-41-HA nanocomposite (temperature 180° C and rotational speed of 100 rpm).

The differences in the crystalline structures were determined by X-ray diffraction. The X-ray patterns of neat PP and PP/MCM-41-HA nanocomposites at rotor rotational speeds of 50 and 100 rpm and chamber temperature of 180° C are shown in Figure 7. The intense peaks that appear at $2\theta = 14.1°$, $2\theta = 16.9°$, $2\theta = 18.6°$, and $2\theta = 21.2°$ are the reflections of (110), (040), (130), and (111) planes, respectively. The next peak at $2\theta = 21.9°$ corresponds to (131) and (041) planes. This structure matches α monoclinic form of isotactic PP [29, 30]. As shown in Fig 7, the position of the peaks remained the same for all samples, but the presence of fillers within the

PP/MCM-41-HA nanocomposites cause the intensities to become lower. This decrease is more obvious in samples that were prepared at 100 rpm when compared to the 50 rpm samples. Diffusive processes improved with increasing the rotor rotational speed, so the possibility of collision X-ray diffractions with the fillers increased, while the intensity of the PP crystalline structure peaks became lower. The XRD image shows that additions of MCM-41/HA nanoparticles have little effect on the crystallization of neat PP.
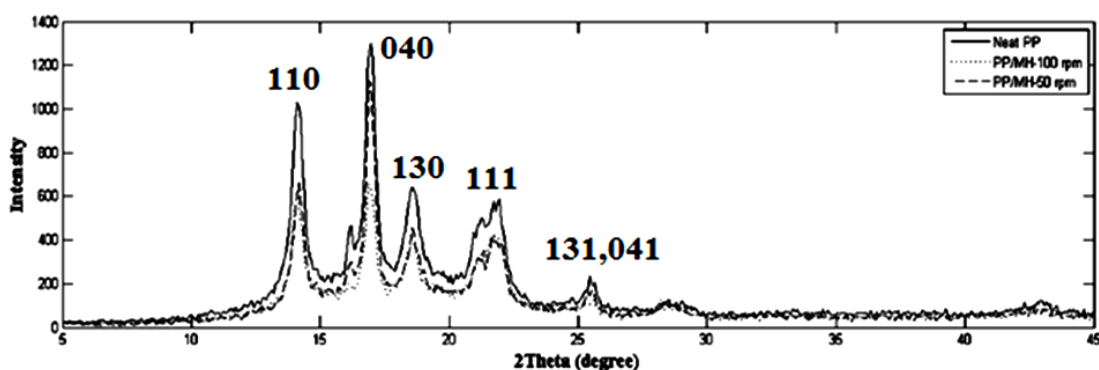

Figure 7. XRD patterns of the neat PP and PP/MCM-41-HA nanocomposite.

4. Conclusion

This work showed the significance of adding MCM-41-HA nanoparticles in addition to specific processing conditions that enhanced the mechanical properties of the nanoparticle material over those of neat PP. Considering the different processing conditions, the results showed that the shear stress exerted on the polymer had a significant influence on the extent of intercalation. The best results for the mechanical properties, torque diagram, and morphological characteristics were achieved using processing conditions that maximized shear stress, at the higher rotational speed of 100 rpm and a chamber temperature of 180° C. According to the torque diagram, the mixing time of 3 min was the best amount of mixing time. This mixing time was the minimum time that allowed for a completed mixing process, saving time and energy.

The PP/MCM-41-HA nanocomposites showed a sensible enhancement of the materials' mechanical properties in comparison with neat PP. The porosity of MCM-41-HA nanoparticles was an exclusive property that caused a chain of the polymeric matrix within the channels, which restrained the agglomeration of MCM-41-HA particles. Tensile and flexural properties of PP/MCM-41-HA nanocomposites were calculated in this paper for the first time. The optimum melt mixing conditions can be used to adjust

the mixing temperatures and rotor speed of the extruder to obtain even better samples.

References

[1] Wei L, Hu N, Zhang Y. Synthesis of Polymer-Mesoporous Silica Nanocomposites. *Mater* 2010; 3(7): 4066-79.
[2] Beck JS, Vartuli JC, Roth WJ, Leonowicz ME, Kresge CT, Schmitt KD, Chu CTW, Olson DH, Sheppard EW. A New Family of Mesoporous Molecular Sieves Prepared with Liquid Crystal Templates. *J Am Chem Soc* 1992; 114(27): 10834-43.
[3] Huo Q, Margolese DI, Ciesla U, Feng P, Gier TE, Sieger P, Leon R, Petroff P, Schuth F, Stucky GD. Generalized Syntheses of Periodic Surfactant/Inorganic Composite Materials. *Nat* 1994; 368(6469): 317-21.
[4] Mokaya R, Jones W. Aluminosilicate Mesoporous Molecular Sieves with Enhanced Stability Obtained by Reacting MCM-41 with Aluminium Chlorohydrate. *Chem Commun* 1998; 7(17): 1839-40.
[5] Wang N, Zhao C, Shi Z, Shao Y, Li H, Gao N. Co-Incorporation of MMT and MCM-41 Nanomaterials Used as Fillers in PP Composite. *Mater Sci Eng B* 2009; 157(1-3): 44-7.

[6]   Liu Y, Wang M. Fabrication and Characteristics of Hydroxyapatite Reinforced Polypropylene as a Bone Analogue Biomaterial. *J Appl Polym Sci* 2007; 106(4): 2780-90.

[7]   Younesi M, Baharololoom ME. Effect of Molecular Weight, Particle Size and Ringer's Solution on Mechanical Properties of Surface-treated Polypropylene-Hydroxyapatite Biocomposites. *J Compos Mater* 2010; 44(24): 2785-99.

[8]   Younesi M, Bahrololoom ME. Formulating the Effects of Applied Temperature and Pressure of Hot Pressing Process on the Mechanical Properties of Polypropylene-Hydroxyapatite Bio-Composites by Response Surface Methodology. *Mater Des* 2010; 31(10): 4621-30.

[9]   Li K, Tjong SC. Preparation and Characterization of Isotactic Polypropylene Reinforced with Hydroxyapatite Nanorods. *J Macromol Sci B* 2011; 50(10): 1983-95.

[10] Modesti M, Lorenzetti A, Bon D, Besco S. Thermal Behaviour of Compatibilised Polypropylene Nanocomposite: Effect of Processing Conditions. *Polym Degrad Stab* 2006; 91(4): 672-80.

[11] Ryu SH, Chang YW. Factors Affecting the Dispersion of Montmorillonite in LLDPE Nanocomposite. *Polym Bull* 2005; 55(5): 385-92.

[12] Vermogen A, Masenelli-Varlot K, Seguela R, Duchet-Rumeau J, Boucard S, Prele P. Evaluation of the Structure and Dispersion in Polymer-Layered Silicate Nanocomposites. *Macromol* 2005; 38(23): 9661-9.

[13] Lertwimolnun W, Vergnes B. Influence of Compatibilizer and Processing Conditions on the Dispersion of Nanoclay in a Polypropylene Matrix. *Polym* 2005; 46(10): 3462-71.

[14] Furlan LG, Ferreira CI, Castel CD, Santos KS, Mello ACE, Liberman SA, Oviedo MAS, Mauler RS. Effect of Processing Conditions on the Mechanical and Thermal Properties of High-Impact Polypropylene Nanocomposites. *Mater Sci Eng A* 2011; 528(22-23): 6715-8.

[15] Al-Malaika S, Sheena H, Fischer D, Masarati E. Influence of Processing and Clay Type on Nanostructure and Stability of Polypropylene-Clay Nanocomposites. *Poly Degrad Stab* 2013; 98(12): 2400-10.

[16] Luijsterburg BJ, Kort GW, Drongelen M, Govaert LE, Goossens JGP. Fast cooling of (non)-nucleated virgin and recycled poly (propylenes): Effect of processing conditions on structural and mechanical properties. *Thermochimica Acta* 2014; 603:94–102.

[17] Macadeo S, Lafranche E, Martins C, Douchain C, Loux C, Krawczak P. Thin wall injection-overmoulding of polyamide 6/polypropylene multilayer parts: influence of processing conditions on thermomechanical properties of the layer assembly. *Int J Mater Prod Technol* 2016; 52(1-2): 53-75.

[18] Delva L, Rageart K, Allear K, Gaspar-Cunha A, Degrieck J, Cardon L. Influence of twin-screw configuration on the mechanical and morphological properties of polypropylene-clay composites. *Int J Mater Prod Technol* 2016; 52(1-2): 176-92.

[19] Motamedi P, Bagheri R. Modification of nanostructure and improvement of mechanical properties of polypropylene/polyamide 6/layered silicate ternary nanocomposites through variation of processing rout. *Compos Part B: Eng* 2016; 85: 207-15.

[20] Caelers HJM, Govaert LE, Peters GWM. The prediction of mechanical performance of isotactic polypropylene on the basis of processing conditions. *Polym* 2016; 83: 116-28.

[21] Yousefpour M, Taherian Z. The Effects of Ageing Time on the Microstructure and Properties of Mesoporous Silica-Hydroxyapatite Nanocomposite. *Superlattices Microstruct* 2013; 54(1): 78-86.

[22] Diaz A, Lopez T, Manjarrez J, Basaldella E, Martinez-Blanes JM, Odriozola JA. Growth of Hydroxyapatite in a Biocompatible Mesoporous Ordered Silica. *Acta Biomater* 2006; 2(2): 173-9.

[23] Sousa A, Souza KC, Sousa EM. Mesoporous Silica/Apatite Nanocomposite: Special Synthesis Route to Control Local Drug Delivery. *Acta Biomater* 2008; 4(3): 671-9.

[24] Saha MC, Kabir MD, Jeelani S. Enhancement in Thermal and Mechanical Properties of Polyurethane Foam Infused with Nanoparticles. *Mater Sci Eng A* 2008; 479(1-2): 213-22.

[25] Wang N, Gao N, Jiang S, Fang Q, Chen E. Effect of Different Structure MCM-41 Fillers with PP-g-MA on Mechanical and Crystallization Performances of Polypropylene. *Compos Part B* 2011; 42(6): 1571-7.

[26] Ji X, Hampsey JE, Hu Q, He J, Yang Z, Lu Y. Mesoporous Silica-Reinforced Polymer Nanocomposites. *Chem Mater* 2003; 15(19): 3656-62.

[27] Wang N, Fang Q, Shao Y, Zhang J. Microstructure and Properties of Polypropylene Composites Filled with Co-Incorporation of MCM-41(with Template) and OMMT Nanoparticles Prepared by Melt-Compounding. *Mater Sci Eng A* 2009; 512(1-2): 32-8.

[28] Li K, Tjong SC. Preparation and Mechanical and Tribological Properties of High-Density Polyethylene/Hydroxyapatite Nanocomposites. *J of Macromol Sci B* 2011; 50(7): 1325-37.

[29] Weidinger A, Hermans PH. On the Determination of the Crystalline Fraction of Isotactic Polypropylene from X-Ray Diffraction. *Macromol Chem Phys* 1961; 50(1): 98-115.

[30] Alexander LE, **X-Ray Diffraction Methods in Polymer Science.** New York: Wiely; 1969.